Available online at www.sciencedirect.com
ScienceDirect
Fluid Phase Equilibria 255 (2007) 167–178
FLUID PHASE EQUILIBRIA
www.elsevier.com/locate/fluid

Evaluation of COSMO-RS for the prediction of LLE and VLE of alcohols + ionic liquids

Mara G. Freire [a], Luís M.N.B.F. Santos [b], Isabel M. Marrucho [a], João A.P. Coutinho [a,*]

[a] *CICECO, Departamento de Química, Universidade de Aveiro, 3810-193 Aveiro, Portugal*
[b] *CIQ, Departamento de Química, Faculdade de Ciências da Universidade do Porto, R. Campo Alegre 687, 4169-007 Porto, Portugal*

Received 5 March 2007; received in revised form 12 April 2007; accepted 17 April 2007
Available online 21 April 2007

Abstract

The huge number of possible combinations of binary mixtures of alcohols and ionic liquids (ILs) make the exhaustive measurement of all these systems impracticable requiring the use of a predictive model for their study. In this work, the predictive capability of COSMO-RS, a model based on unimolecular quantum chemistry calculations, was evaluated for the description of the liquid–liquid equilibria and the vapour–liquid equilibria of binary mixtures of alcohols and several imidazolium and pyridinium-based ILs. The effect of the ions and alcohols conformers on the quality of the predictions was assessed and the quantum chemical COSMO calculation at the BP/TZVP level derived from the lower energy conformations was adopted. Although a degradation in the liquid–liquid equilibria predictions with increasing size length of the alkyl chain of the alcohol or of the ionic liquid and with the short chain alcohol methanol in the vapour–liquid equilibria predictions were observed, in general a reasonable qualitative agreement between the model predictions and experimental data for a large combination of structural variations of both alcohols and ILs was obtained. COSMO-RS can thus be very useful in the scanning of the growing number of known ILs to find suitable candidates, or help designing new ILs, for specific applications before extensive experimental measurements.

Keywords: Ionic liquids; Alcohols; LLE; VLE; COSMO-RS

1. Introduction

Room temperature ionic liquids have received recently increased interest as potential "green" solvents replacements for volatile organic solvents essentially due to their negligible vapour pressures [1]. Ionic liquids are typically salts composed of relatively large organic cations and inorganic or organic anions and the presence of these large ions tend to reduce the lattice energy of the crystalline structure lowering their melting point, and thus they generally remain liquid at or near room temperature. Among their unique characteristics they present the potential to tune their physical and chemical properties by varying different features of the ionic liquid, including the alkyl chain length on the cation and the anion, and a detailed knowledge of the impact of the different structural changes on the properties of ILs will enable their use as "designer solvents".

Among the several applications foreseeable for ionic liquids in the chemical industry such as solvents in organic synthesis, as homogeneous and biphasic transfer catalysts, and in electrochemistry, there has been considerable interest in the potential

Abbreviations: [C_2mim][Tf_2N], 1-ethyl-3-methylimidazolium bis(trifluoromethylsulfonyl)imide; [C_4mim][BF_4], 1-butyl-3-methylimidazolium tetrafluoroborate; [C_4mim][PF_6], 1-butyl-3-methylimidazolium hexafluorophosphate; [C_4mim][Tf_2N], 1-butyl-3-methylimidazolium bis(trifluoromethylsulfonyl)imide; [C_5mim][PF_6], 1-pentyl-3-methylimidazolium hexafluorophosphate; [C_6mim][BF_4], 1-hexyl-3-methylimidazolium tetrafluoroborate; [C_6mim][PF_6], 1-hexyl-3-methylimidazolium hexafluorophosphate; [C_6mim][Tf_2N], 1-hexyl-3-methylimidazolium bis(trifluoromethylsulfonyl)imide; [C_7mim][PF_6], 1-heptyl-3-methylimidazolium hexafluorophosphate; [C_8mim][BF_4], 1-octyl-3-methylimidazolium tetrafluoroborate; [C_8mim][PF_6], 1-octyl-3-methylimidazolium hexafluorophosphate; [C_8mim][Tf_2N], 1-octyl-3-methylimidazolium bis(trifluorosulfonyl)imide; [C_3C1mim][Tf_2N], 2,3-dimethyl-1-propylimidazolium bis(trifluoromethylsulfonyl)imide; [C_6C_1mim][Tf_2N], 2,3-dimethyl-1-hexylimidazolium bis(trifluoromethylsulfonyl)imide; [C_6py][Tf_2N], 1-*n*-hexylpyridinium bis(trifluoromethylsulfonyl)imide; [C_4mpy][BF_4], 1-*n*-butyl-3-methylpyridinium tetrafluoroborate; [C_4mpy][Tf_2N], 1-*n*-butyl-3-methylpyridinium bis(trifluoromethylsulfonyl)imide; [C_6mpy][Tf_2N], 1-*n*-hexyl-3-methylpyridinium bis(trifluoromethylsulfonyl)imide; [C_1mim][$(CH_3)_2PO_4$], 1,3-dimethylimidazolium dimethylphosphate; [C_4mim][OctS], 1-butyl-3-methylimidazolium octylsulfate

* Corresponding author. Tel.: +351 234 370200; fax: +351 234 370084.
E-mail address: jcoutinho@dq.ua.pt (J.A.P. Coutinho).

0378-3812/$ – see front matter © 2007 Elsevier B.V. All rights reserved.
doi:10.1016/j.fluid.2007.04.020

of ILs for separation processes as extraction media [2–5]. In particular, it was already shown that ILs can be successfully used for the extraction of ethanol and butanol from aqueous fermentation broths [4], and for the extraction of alcohols from alcohol/alkane mixtures [5]. Furthermore, when ILs are used as solvents for reactions or as catalysts or catalysis medium in the presence of alcohols products or reactants, reliable thermodynamic data on such systems are of great importance for the design of more efficient and possibly greener industrial processes.

The development of ILs specifically designed for a particular reaction or separation process requires a large data bank on pure ILs physical properties and on their phase behaviour with common solvents. A fair amount of data for solid-liquid equilibria (SLE), liquid–liquid equilibria (LLE) and vapour–liquid equilibria (VLE) of binary systems for various ILs and alcohols have already been reported [6–31]. As it is unfeasible to experimentally measure the phase behaviour of all the possible combinations of anions and cations in ILs with all the possible alcohols, it is essential to make measurements on selected systems to provide results that can be used to develop correlations and to test predictive methods. Several models have been attempted for correlating experimental data of ILs systems phase equilibria. Based on excess free Gibbs energy models, Wilson, UNIQUAC and original and modified UNIFAC equations have been applied to correlate SLE and VLE of ILs [16–18,23–25]. In particular original and modified UNIFAC was also applied to correlate activity coefficients at infinite dilution and excess molar enthalpies of systems involving ILs [25]. Another local composition model that proved being able to correlate data of ILs systems was the non-random two-liquid (NRTL), that was applied to both VLE and LLE systems [5,8,23,26–31]. A different approach was proposed by de Sousa and Rebelo [32] that used a "polymer-like" modified Flory–Huggins equation to correlate the LLE of ILs solutions, because of the similarity between the LLE phase diagrams of polymer solutions and those of IL solutions. Nevertheless, correlations are limited in scope and group contribution methods are not a good alternative due to the lack of IL group parameters at present. On the other hand, the use of equations of state (EoS) requires the ILs critical parameters or vapour pressures, which are not directly measurable and thus must be obtained indirectly [33,34]. In addition, EoS methods for complex mixtures are not fully predictive requiring knowledge of the phase equilibrium at least, at one mixture composition, for binary parameter fitting.

COSMO-RS (Conductor-like Screening Model for Real Solvents) is a novel method for the prediction of thermophysical properties of fluids based on unimolecular quantum calculations and is an alternative to the structure-interpolating group-contribution methods (GMCs) [35–38]. This method is therefore, able to describe, at least qualitatively, structural variations correctly. A few works dealing with the application of COSMO-RS to the description of LLE of ILs and alcohols, hydrocarbons, ethers, ketones or water systems were previously done [19–22,39,40]. Also, the VLE binary systems description of ILs and alcohols, hydrocarbons, ketones or water using COSMO-RS and COSMO-RS(Ol) was previously attempted [25,40,41]. Previous contributions dealing with mixtures of ILs and alcohols are, however, of limited scope and do not allow the evaluation of the applicability and reliability of the method to those systems. In this work, a systematic study for a large combination of structural variations of both ILs and alcohols was carried out. Although with a different aim, it should be also mentioned the work of Sahandzhieva et al. [22] were a comparison of several COSMO-RS versions provided by the COSMOtherm software package (versions C1.2, release 01.03 and 05.02 and version 2.1, release 01.04) in the prediction of the [bmim][PF_6]-butan-1-ol system LLE is presented. The objective here is to evaluate the potential of COSMO-RS in the prediction of liquid–liquid and vapour–liquid phase equilibrium of binary systems containing ILs and alcohols using the more recent version 2.1, release 01.05.

2. Phase equilibria prediction of systems involving ILs and alcohols

COSMO-RS as proposed by Klamt and co-workers [35–38], combines the electrostatic advantages and the computational efficiency of the quantum chemical dielectric continuum solvation model, COSMO, with a statistical thermodynamics approach for local interaction of surfaces where the local deviations from dielectric behaviour as well as hydrogen bonding are considered. The standard procedure of COSMO-RS calculations consists essentially in two steps: quantum chemical COSMO calculations for the molecular species involved, where the information about solvents and solutes is extracted, and COSMO-RS statistical calculations performed with the COSMOtherm program [42,43].

In the COSMO calculations, the solute molecules are assumed to be in a virtual conductor environment, where the solute molecule induces a polarization charge density, σ, on the interface between the molecule and the conductor. These charges act back on the solute and generate a more polarized electron density than in vacuum. In the quantum chemical self-consistency algorithm cycle, the solute molecule is converged to its energetically optimal state in a conductor with respect to electron density. The calculations end up with the self-consistent state of the solute in the presence of a virtual conductor that surrounds the solute outside the cavity. Although time-consuming, one advantage of this procedure is that the quantum chemical calculations have to be performed just once for each molecule of interest.

The deviations of the real fluids behaviour, ILs and alcohols, with respect to an ideal conductor are taken into account, and the electrostatic energy differences and hydrogen bonding energies are quantified as functions of the local COSMO polarization charge densities σ and σ' of the interacting surface of the molecule divided into segments. The 3D polarization density distribution on the surface of each molecule X_i is converted into a distribution function, the σ-profile, $p^{X_i}(\sigma)$, that describes the polarity of each surface segment on the overall surface of the molecule. If a mixture is considered, the σ-profile of a solvent S, $p_S(\sigma)$, is the result of adding the individual $p^{X_i}(\sigma)$ weighed

by their mole fractions, x_i, as expressed in Eq. (1):

$$p_S(\sigma) = \sum_{i \in S} x_i p^{X_i}(\sigma) \quad (1)$$

For the statistical thermodynamics is expedient to consider a normalized ensemble and since the integral of $p^{X_i}(\sigma)$ over the entire σ-range is the total surface area A^{Xi} of a compound X_i, the normalised σ-profile, $p'_S(\sigma)$, of the overall system is defined as follows

$$p'_S(\sigma) = \frac{p_S(\sigma)}{A_S} = \frac{p_S(\sigma)}{\sum_{i \in S} x_i A^{X_i}} \quad (2)$$

The electrostatic misfit energy (E_{misfit}) and hydrogen bonding (E_{HB}) are described as functions of the polarization charges of the two interacting segments, σ and σ' or $\sigma_{acceptor}$ and σ_{donor}, if the segments are located in a hydrogen bond donor or acceptor atom, as described in Eqs. (3) and (4). The van der Waals energy (E_{vdW}) is dependent only on the elements of the atoms involved and is described by Eq. (5):

$$E_{misfit}(\sigma, \sigma') = a_{eff} \frac{\alpha'}{2} (\sigma + \sigma')^2 \quad (3)$$

$$E_{HB} = a_{eff} c_{HB} \min(0; \min(0; \sigma_{donor} + \sigma_{HB}) \times \max(0; \sigma_{acceptor} - \sigma_{HB})) \quad (4)$$

$$E_{vdW} = a_{eff}(\tau_{vdW} + \tau'_{vdW}) \quad (5)$$

where α' is the coefficient for electrostatic misfit interactions, a_{eff} is the effective contact area between two surface segments, c_{HB} is the coefficient for hydrogen bond strength, σ_{HB} is the threshold for hydrogen bonding and τ_{vdW} and τ'_{vdW} are element-specific vdWs coefficients.

The most important descriptor used in COSMO-RS is in fact the local screening charge density, σ, which would be induced on the molecular surface if the molecule would be embedded in a virtual conductor. This descriptor can be calculated by quantum chemical programs using the continuum solvation model COSMO, and it is an extremely valuable descriptor for the local polarity of molecular surface and it is the only descriptor determining the interaction energies. Thus, the ensemble of surface pieces characterising a liquid system S is described by the distribution function, $p_S(\sigma)$, that depicts the amount of surface in the ensemble having a screening charge density between σ and $\sigma + d\sigma$. Thus, the σ-profile of a single compound is derived from the quantum chemical COSMO output for that molecule, applying some local averaging algorithm that take into account that only screening charge densities averaged over an effective contact area are of physical meaning in COSMO-RS [42,43].

The molecular interactions in the solvent are thus fully described by $p_S(\sigma)$ and the chemical potential differences resulting from these interactions are calculated with an exact statistical thermodynamics algorithm for independently pair-wise interacting surfaces [42,43]. The COSMO-RS method depends only on a small number of adjustable parameters (predetermined from known properties of individual atoms) and that are not specific for functional groups or type of molecules. Moreover, statistical thermodynamics enables the determination of the chemical potential of all components in the mixture and, from these, the thermodynamic properties can be derived.

The approach to a pseudobinary mixture was used to calculate the LLE and VLE of mixtures of an ionic liquid and an alcohol, considering the cation and the anion of the IL as separate compounds with the same mole fraction. The chemical potentials are then calculated for each ternary system (anion + cation + alcohol), where the chemical potential of the whole IL is the sum of the chemical potentials of both the cation and anion. For LLE phase diagrams calculations, a numerical approach is used to find the compositions of equal chemical potentials at a fixed temperature.

The ILs + alcohols binary systems phase equilibria was studied using the quantum chemical COSMO calculation performed in the Turbomole program package [44,45] using the BP density functional theory and the Ahlrichs-TZVP (triple-ζ valence polarized large basis set) [46] using the fully optimized geometries at the same level of theory for the lower energy conformers of each cation, anion and alcohol.

3. LLE and VLE experimental database

Experimental liquid–liquid and vapour–liquid equilibria binary systems data of several common alcohols + imidazolium and alcohols + pyridinium-based ILs were taken from literature and are summarized in Table 1.

4. Results and discussion

Prior to extensive comparisons between COSMO-RS predictions and the experimental data available, a study concerning different energy conformers of both ions and alcohols were compared to access the best conditions of the COSMO-RS predictions in regard to the experimental data. All the COSMO-RS calculations therein after were carried at the BP/TZVP (Turbomole [44,45], DFT/COSMO calculation with the BP functional and TZVP [46] basis set using the optimized geometries at the same level of theory) with the parameter file BP_TZVP_C21_0105.

4.1. Conformers influence

To study the influence of the different anions, cations and alcohols conformations on the COSMO-RS LLE and VLE binary systems predictions, stable conformers with different COSMO energies have been used. Fig. 1 presents an example of the conformers influence in the COSMO-RS predictions for the binary liquid–liquid equilibria between [C_2mim][Tf_2N] and butan-1-ol and the comparison with the experimental data. In this case there are three different energy states for the cation, two for the anion and two for the butan-1-ol that are a result of torsional rotations. The lowest energy conformation of cation and/or anion and/or alcohol provide the best qualitative description of the overall phase behaviour as found previously in water + IL binary systems [40]. In the example presented, the predictions deviate

Table 1
Experimental LLE and VLE IL + alcohol binary systems

IL	Alcohol	Type of equilibria	Reference
$[C_2mim][Tf_2N]$	Propan-1-ol Butan-1-ol Pentan-1-ol	LLE	[6,15]
$[C_4mim][BF_4]$	Propan-1-ol Butan-1-ol Hexan-1-ol Propan-2-o Butan-2-ol Isobutanol *tert*-Butanol	LLE	[6,21]
$[C_4mim][PF_6]$	Ethanol Propan-1-ol Butan-1-ol	LLE	[9,20–22,29]
$[C_4mim][Tf_2N]$	Butan-1-ol Hexan-1-ol Isobutanol	LLE	[6,9,11]
$[C_5mim][PF_6]$	Butan-1-ol	LLE	[21]
$[C_6mim][BF_4]$	Butan-1-ol Hexan-1-ol Octan-1-ol	LLE	[6,7]
$[C_6mim][PF_6]$	Butan-1-ol	LLE	[21]
$[C_6mim][Tf_2N]$	Butan-1-ol Pentan-1-ol Hexan-1-ol Octan-1-ol	LLE	[7,12,13]
$[C_7mim][PF_6]$	Butan-1-ol	LLE	[21]
$[C_8mim][BF_4]$	Pentan-1-ol Hexan-1-ol Octan-1-ol	LLE	[7,13]
$[C_8mim][PF_6]$	Butan-1-ol	LLE	[21]
$[C_8mim][Tf_2N]$	Octan-1-ol	LLE	[7]
$[C_3C_1mim][Tf_2N]$	Butan-1-ol Hexan-1-ol	LLE	[6]
$[C_6C_1mim][Tf_2N]$	Hexan-1-ol	LLE	[7]
$[C_6py][Tf_2N]$	Hexan-1-ol	LLE	[8]
$[C_4mpy][BF_4]$	Propan-1-ol Butan-1-ol	LLE	[8]
$[C_4mpy][Tf_2N]$	Butan-1-ol Hexan-1-ol	LLE	[8]
$[C_6mpy][Tf_2N]$	Hexan-1-ol	LLE	[8]
$[C_1mim][(CH_3)_2PO_4]$	Methanol Ethanol	VLE	[24]
$[C_2mim][Tf_2N]$	Methanol Ethanol Propan-2-ol	VLE	[24,25]
$[C_4mim][Tf_2N]$	Methanol Ethanol Propan-1-ol Propan-2-ol	VLE	[24,31]
$[C_6mim][Tf_2N]$	Methanol Ethanol	VLE	[25]
$[C_8mim][BF_4]$	Methanol Ethanol Propan-1-ol	VLE	[26]
$[C_4mim][OctS]$	Methanol Ethanol Propan-1-ol	VLE	[26]

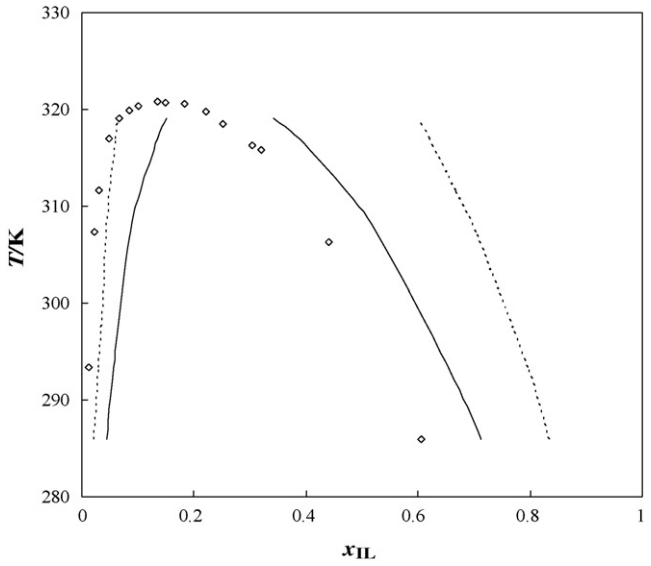

Fig. 1. Liquid–liquid phase diagram for $[C_2mim][Tf_2N]$ with butan-1-ol: (◊) experimental data [14]; (—) COSMO-RS prediction calculations with the lowest energy conformers; (- - -) COSMO-RS prediction calculations with higher energy conformers.

slightly in the alcohol rich-phase but poorer results are obtained in the IL-rich phase due to the higher solubilities of alcohols in ILs. A more detailed analysis involving the distribution coefficients of the alcohol in both phases can be accessed in the Supporting Information, were it is proved that the lower energy conformers used provide the best qualitative and quantitative predictions in respect to the experimental results. This trend was observed for almost all the binary systems analysed and thus the lowest energy isomers conformation for all the species involved will be used in the COSMO-RS calculations below, since the main goal of this contribution is to analyse the structural modifications of both ions and alcohols and to test the COSMO-RS predictive ability.

4.2. Liquid–liquid equilibria prediction

The quantum chemical COSMO descriptions of the pure ILs and alcohols were achieved using the BP functional and the triple-ζ valence polarized large basis set (TZVP) and the liquid–liquid calculations were then performed using the pseudobinary approach described above. The results obtained with the COSMO-RS calculations are compared with T–x_{IL} experimental data in Figs. 2–12.

All systems involving ILs and alcohols show nearly symmetrical binodal curves when the results are plotted against the mass fraction. Using mole fractions as concentration units, shifts the maximum upper critical solution temperature (UCST) to the lower IL concentrations because of the large differences in molecular weights between the ILs and alcohols, resulting in asymmetrical curves.

To study the impact of structural variations in the ILs anions and cations and in the alcohols on the predicted phase diagrams the mole fraction basis was adopted. The results obtained are discussed below from different perspectives to evaluate the

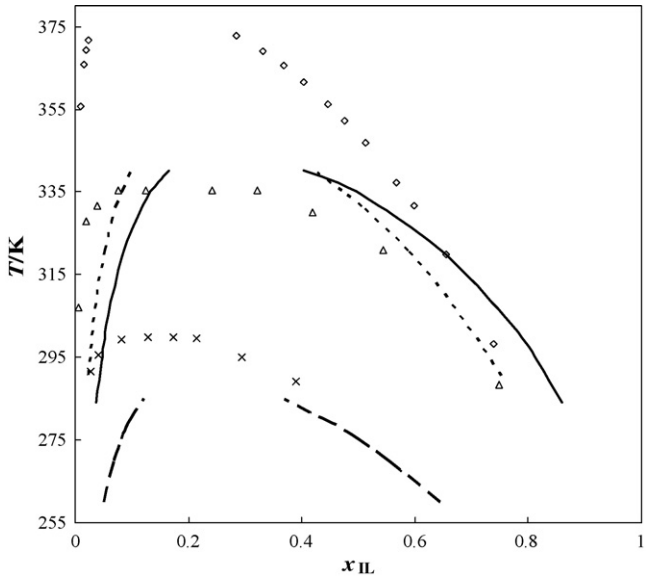

Fig. 2. Liquid–liquid phase diagram for [C_4mim][PF_6] (◊) (—), [C_4mim][BF_4] (△) (- - -) and [C_4mim][Tf_2N] (×) (– – –) with butan-1-ol. The single symbols and the lines represent respectively the experimental data [6,21] and the COSMO-RS prediction calculations.

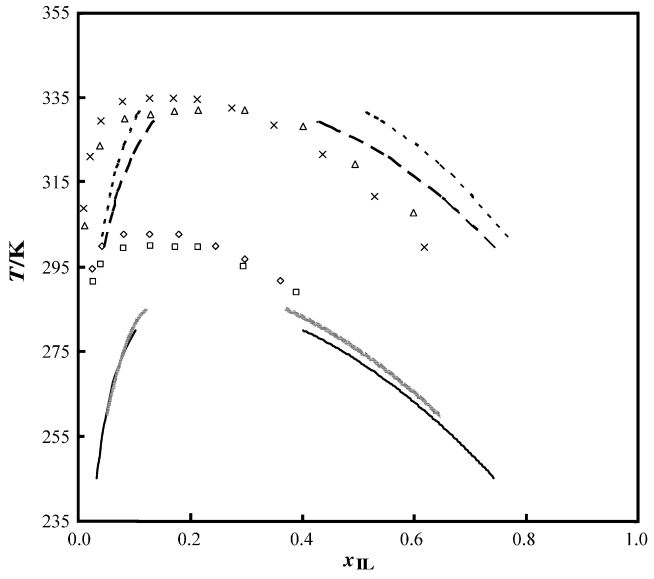

Fig. 4. Liquid–liquid phase diagram for [C_4mim][Tf_2N] (□) (wwww) and [C_4mpy][Tf_2N] (◊) (—) with butan-1-ol, and [C_4mim][Tf_2N] (△) (- - -) and [C_4mpy][Tf_2N] (×) (– – –) with hexan-1-ol. The single symbols and the lines represent respectively the experimental data [6,8] and the COSMO-RS prediction calculations.

COSMO-RS predictive capability to describe the mutual solubilities in the liquid phase.

4.2.1. Anion identity influence

The influence of the anion was examined by changing it on a number of systems, while keeping the cation and the alcohol, as depicted in Fig. 2. This figure presents a comparison between experimental data and COSMO-RS predictions for the liquid–liquid phase behaviour of butan-1-ol and the [C_4mim] cation in combination with three different anions: [Tf_2N], [BF_4] and [PF_6]. Experimentally, the anion has a marked effect on the phase behaviour of imidazolium-based and pyridinium-based ILs with alcohols. A reasonable qualitative prediction was obtained for the entire liquid–liquid phase diagram of [C_4mim][BF_4] and [C_4mim][Tf_2N] with butan-1-ol, although the alcohol-rich phase predictions deviate strongly from experimental results. On the IL-rich phase, COSMO-RS is able to predict the increasing alcohol solubility with the anion, failing however in providing the correct variation of the IL solubility

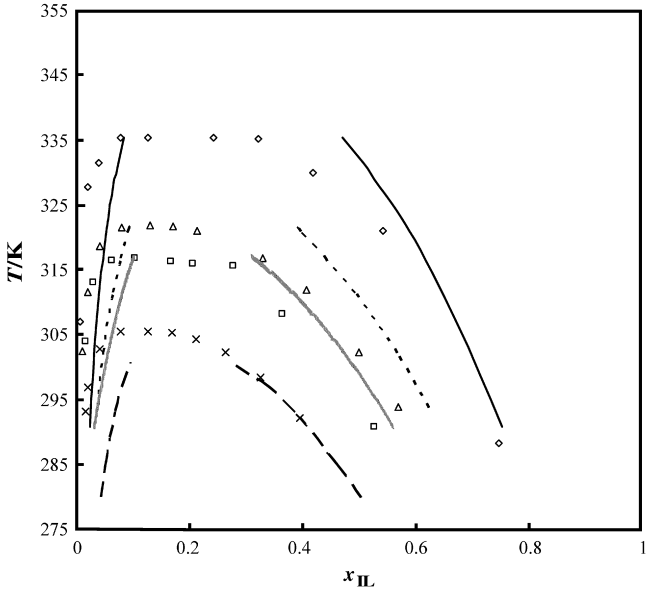

Fig. 3. Liquid–liquid phase diagram for [C_4mim][BF_4] (□) (wwww) and [C_4mpy][BF_4] (×) (– – –) with propan-1-ol, and [C_4mim][BF_4] (◊) (—) and [C_4mpy][BF_4] (△) (—) with butan-1-ol. The single symbols and the lines represent respectively the experimental data [6,8] and the COSMO-RS prediction calculations.

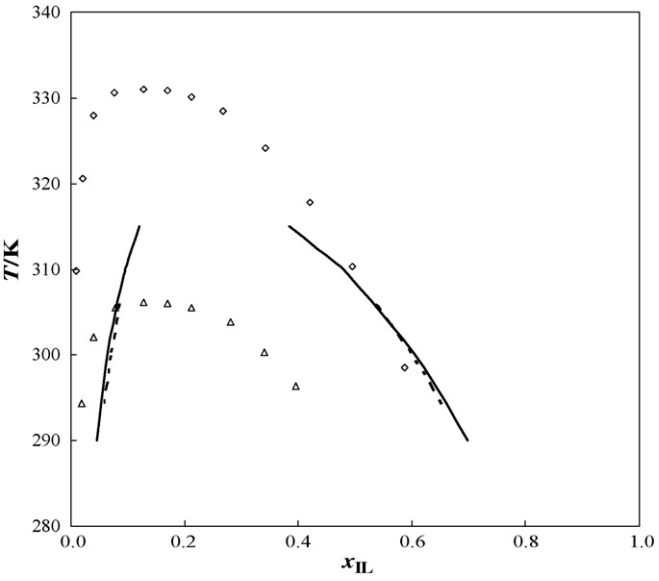

Fig. 5. Liquid–liquid phase diagram for [C_6mim][Tf_2N] (△) (- - -) and [C_6C_1mim][Tf_2N] (◊) (—) with hexan-1-ol. The single symbols and the lines represent respectively the experimental data [7] and the COSMO-RS prediction calculations.

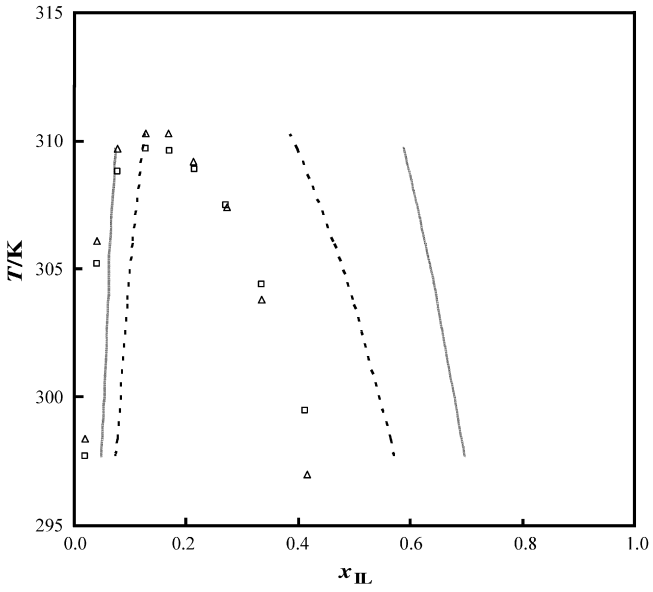

Fig. 6. Liquid–liquid phase diagram for [C_6py][Tf_2N] (□) (wwww) and [C_6mpy][Tf_2N] (△) (- - -) with hexan-1-ol. The single symbols and the lines represent respectively the experimental data [8] and the COSMO-RS prediction calculations.

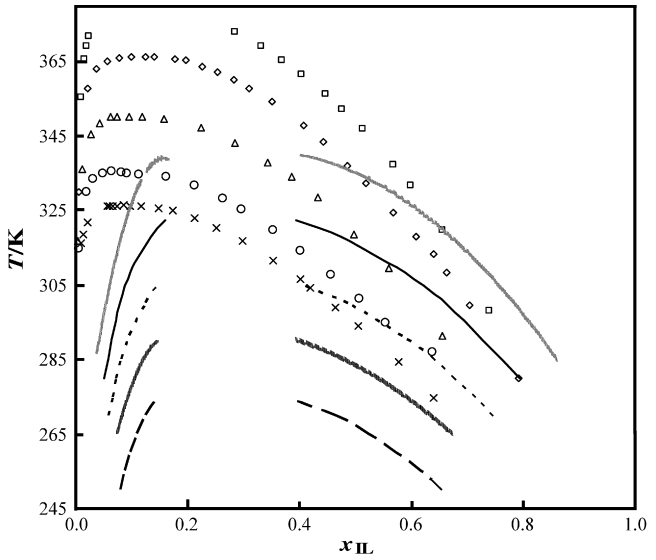

Fig. 8. Liquid–liquid phase diagram for [C_4mim][PF_6] (□) (wwww) [C_5mim][PF_6] (◊) (—), [C_6mim][PF_6] (△) (- - - - - - -), [C_7mim][PF_6] (◯) (▬▬) and [C_8mim][PF_6] (×) (– – –) with butan-1-ol. The single symbols and the lines represent respectively the experimental data [21] and the COSMO-RS prediction calculations.

in the alcohol-rich phase between [PF_6] and [BF_4] and thus will fail in the UCST prediction differences due to these two anions. Further similar results for other systems and a representation of the distribution coefficients of the alcohol in both phases are reported in the Supporting Information of this manuscript.

4.2.2. Cation class influence

The influence of the cation on the LLE can be assessed by examination of the experimental phase diagrams of imidazolium and pyridinium-based ILs and their predictions using COSMO-RS as presented in Figs. 3 and 4. In Fig. 3, the anion [BF_4] is retained for both alcohols, propan-1-ol and butan-1-ol, and it can be observed that the UCST is higher for the imidazolium-based ILs than for the pyridinium-based, displaying lower mutual solubilities between the alcohol and the IL at temperatures below the UCST. This trend is well predicted by COSMO-RS for the two alcohols studied with both alcohols and both cation class. Nevertheless, the opposite trend is observed for the experimental phase behaviour of the [Tf_2N]-based ILs, where the UCST is higher for the pyridinium-based

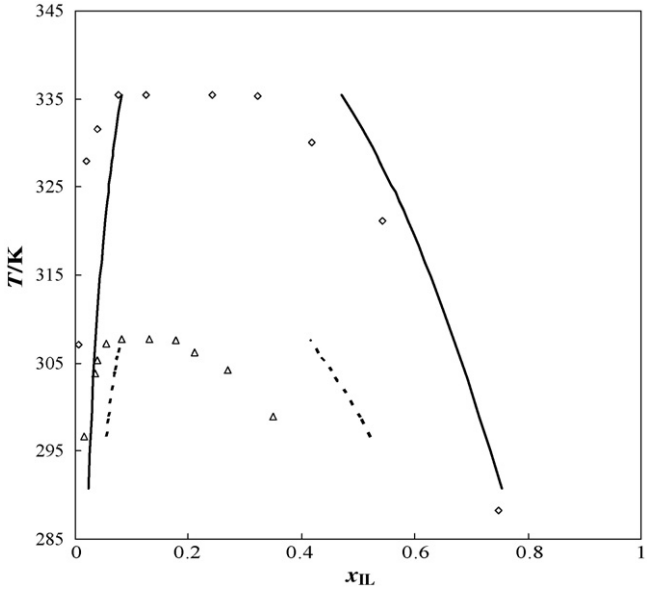

Fig. 7. Liquid–liquid phase diagram for [C_4mim][BF_4] (◊) (—) and [C_6mim][BF_4] (△) (- - -) with butan-1-ol. The single symbols and the lines represent respectively the experimental data [6] and the COSMO-RS prediction calculations.

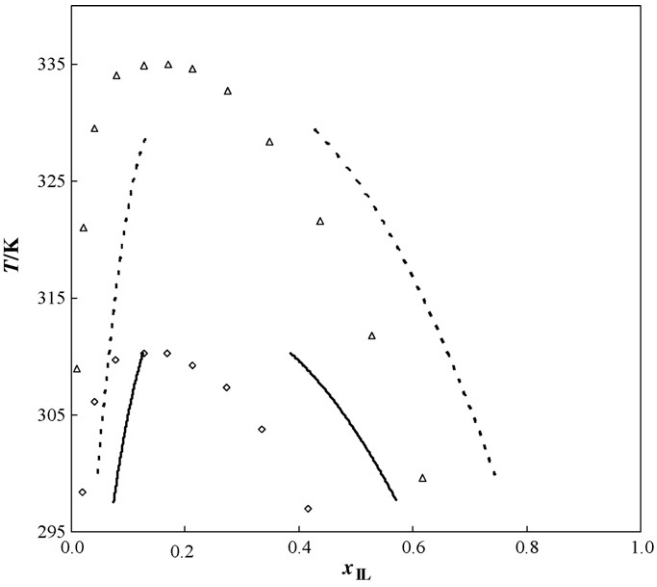

Fig. 9. Liquid–liquid phase diagram for [C_4mpy][Tf_2N] (△) (- - -) and [C_6mpy][Tf_2N] (◊) (—) with hexan-1-ol. The single symbols and the lines represent respectively the experimental data [8] and the COSMO-RS prediction calculations.

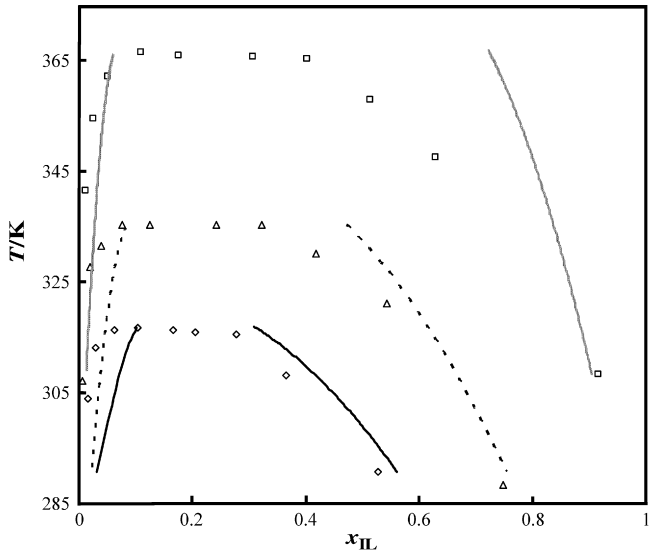

Fig. 10. Liquid–liquid phase diagram for [C_4mim][BF_4] with propan-1-ol (◊) (—), butan-1-ol (△) (- - -) and hexan-1-ol (□) (wwww). The single symbols and the lines represent respectively the experimental data [6] and the COSMO-RS prediction calculations.

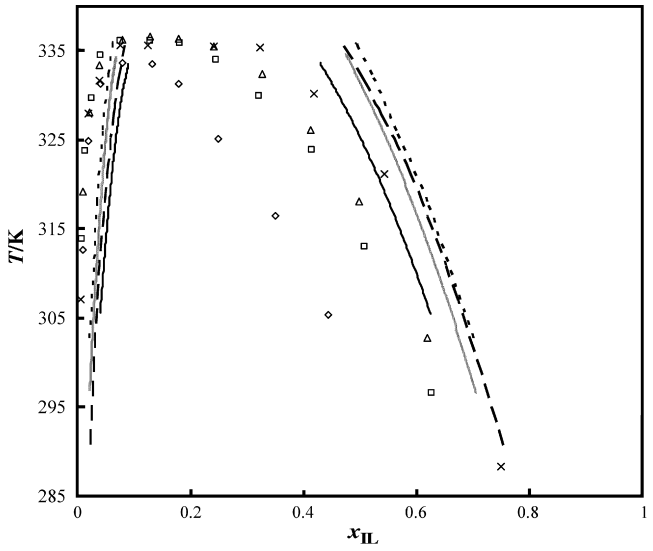

Fig. 12. Liquid–liquid phase diagram for [C_4mim][BF_4] with butan-1-ol (×) (– – –), butan-2-ol (□) (wwww), isobutanol (△) (- - -) and *tert*-butanol (◊) (—). The single symbols and the lines represent respectively the experimental data [6] and the COSMO-RS prediction calculations.

ILs, as shown in Fig. 4. The COSMO-RS predictions capture the same trend for both anions-based ILs while predicting the lower mutual solubilities for the imidazolium-based ILs, assuming that the anion identity will not change the polarity observed due to the cation class, and fails in the prediction of the [Tf_2N]-based ILs behaviour. Results for another similar system and for the alcohol distribution coefficients for the system presented are depicted in the Supporting Information of this manuscript.

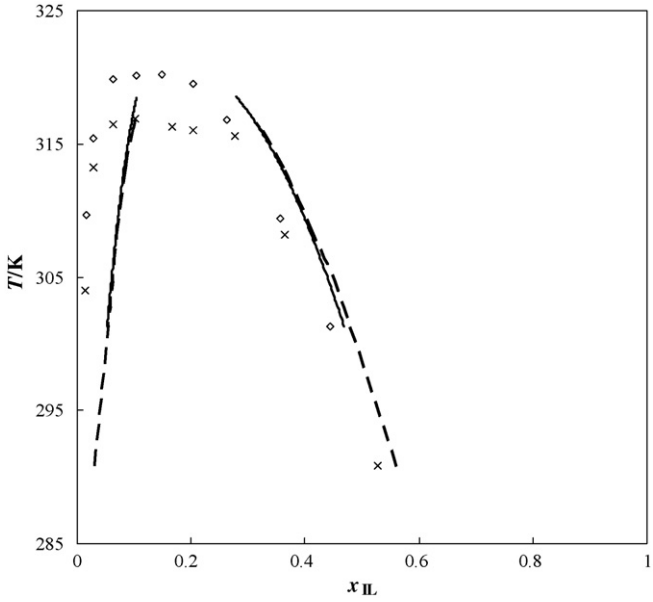

Fig. 11. Liquid–liquid phase diagram for [C_4mim][BF_4] with propan-1-ol (×) (– – –) and propan-2-ol (◊) (—). The single symbols and the lines represent respectively the experimental data [6] and the COSMO-RS prediction calculations.

4.2.3. Cation methyl inclusion influence

Figs. 5 and 6 present the liquid–liquid phase behaviour for hexan-1-ol and two different families of [Tf_2N] based-ILs with different number of substitutions at the cation. The inclusion of a methyl group in both the [C_6mim] and [C_6py] cations (forming [C_6C_1mim] and [C_6mpy]) leads to an UCST increase and decrease of the IL and alcohol mutual solubilities at any particular temperature. This effect is shown in Fig. 5, where the acidic C2 hydrogen of the imidazolium cation is replaced by a methyl group and therefore the ability of hydrogen bonding with the alcohol is greatly reduced. This effect is not as pronounced in the pyridinium-based ILs, as depicted in Fig. 6. In the case of [C_6mim][Tf_2N] and [C_6C_1mim][Tf_2N] the COSMO-RS calculations give approximately the same liquid–liquid phase behaviour for both systems, not distinguishing the experimental differences observed in the mutual solubilities due to the hydrogen-bonding increased ability in the absence of the methyl group. An analysis of the σ-profiles of the imidazolium cations shows no major differences in their polarities, and thus in their hydrogen-bond abilities, which could explain the failure of the COSMO-RS calculations for predicting the differences in the mutual solubilities for [C_6mim][Tf_2N] and [C_6C_1mim][Tf_2N] with hexan-1-ol. On the other hand, for the pyridinium-based ILs, the COSMO-RS calculations fail in estimating the mutual solubilities, predicting a higher UCST for the [C_6py][Tf_2N] than for [C_6mpy][Tf_2N], where experimentally the opposite trend is observed. Although experimentally small deviations in the mutual solubilities between the both pyridinium-based ILs are found, the COSMO-RS predicts considerable differences in their LLE behaviour due to the σ-profiles significant differences in both pyridinium-based ILs. This poor description of both pure ILs class-based is the major reason for the differences obtained in the predictions. A further analysis of the alcohol experimental and predicted distribution coefficients in

both phases is presented in the Supporting Information of this manuscript.

4.2.4. Cation alkyl chain length influence

The influence of the cation alkyl chain length in the IL-alcohol mutual solubilities is presented in Figs. 7–9. Experimentally, it can be observed that as the alkyl chain length of the cation increases the UCST of the system decreases. The mutual solubilities of both IL and alcohol increase at any particular temperature with an increase of the cation alkyl chain length, but a larger enhancement in the solubility occurs in the IL-rich phase when compared to the IL solubility in the alcohol-rich phase. A cation chain length increase leads to an increase in the van der Waals interactions between the hydrophobic chain and the alcohol alkyl portion, thus enhancing the mutual solubilities between the alcohols and ILs and decreasing the UCST.

The prediction by COSMO-RS calculations shows a fair quantitative agreement with the experimental data available. Nevertheless, from the qualitative point of view, the COSMO-RS adequately describes the increase in solubility with the cation alkyl chain length increase, independently of the cation type, alcohol or anion identity. The larger increase in the alcohol solubility in the IL-rich phase when compared to the alcohol rich-phase is also correctly described. For the imidazolium $[PF_6]$-based and $[Tf_2N]$-based ILs shown in Figs. 8 and 9, respectively, the predictions present higher deviations from experimental data compared with the $[BF_4]$-based ILs presented in Fig. 7, but the correct trend of increasing mutual solubilities with alkyl chain length is well described for all the ILs.

However, the predictions show a clear quantitative degradation of the predictions with increasing chain length, or with the IL non-polar character increase. This seems to be one of the most important shortcomings of the COSMO-RS predictions. In a previous work dealing with different ILs and water binary systems [40], this degradation with the IL alkyl chain length increase was not observed and the deviations from experimental data were similar for the entire $[C_2$-C_8mim] series of $[Tf_2N]$-based ILs liquid–liquid equilibria with water. The major reason for the deviations observed with alcohols arises from the underestimation of the van der Waals energy between the alkyl chains of both IL cations and alcohols. Further examples and one example of the alcohol distribution coefficients are presented in the Supporting Information.

4.2.5. Alcohol chain length influence

The data presented in Fig. 10 show an increasing experimental UCST with increasing size of the alkyl chain length of the alcohols for all the ILs considered. The alcohol polar character decreases with increasing chain length makes it more aliphatic, enhancing the tendency of the mixtures to demixing.

The COSMO-RS proved to adequately predict the mutual solubilities tendency for different ILs and alcohols, predicting the UCST increase with the alcohol chain length as shown in Fig. 10. Although a superior quantitative agreement is obtained for the lower alcohols, higher deviations appear with the chain length increase of the alcohols. Both these deviations and those discussed in the previous point resulting from the increase in the cation chain length seem to arise from the IL-alcohol microstructure formation [47] that it is not taken into account by the COSMO-RS calculations. In Fig. 10, the phase diagrams of $[C_4mim][BF_4]$ with three alcohols are presented. The best predictions are obtained for the $[C_4mim][BF_4]$ with propan-1-ol and larger deviations are found for the butan-1-ol and even larger for the hexan-1-ol. The deviations from experimental data are even more pronounced if the combination of long chain alcohols with the longer alkyl chain length cations is considered, as shown in several examples in the Supporting Information. A further analysis of the predicted and experimental alcohol distribution coefficients in both phases supports this predictive degradation with the alcohol chain length increase and it is available in the Supporting Information.

In general, the predictive LLE capacity of COSMO-RS improves with the increasing polarity of the solvent. Domańska et al. [19,39] presented the COSMO-RS predictions for LLE binary systems of ILs with alkanes and ketones where it can be seen that the UCST and mutual solubilities deviations are much larger than those reported in the present work. However, in a previous work by Freire et al. [40], it was shown that the mutual solubilities predictions with COSMO-RS for IL with water systems are much closer of experimental values than the LLE predictions for ILs with alcohols presented here.

4.2.6. Alcohol structural isomers influence

Figs. 11 and 12 present the experimental and the COSMO-RS predictions of the behaviour of $[C_4mim][BF_4]$ with propan-1-ol and propan-2-ol and with butan-1-ol, butan-2-ol, isobutanol and *tert*-butanol. Experimentally the UCST of these systems are almost identical, in particular for the case of the butan-1-ol isomers. For the propan-1-ol isomers the COSMO-RS prediction fails in detecting the differences in mutual solubilities between these isomers, and the same happens for the non-branched isomers, butan-1-ol and butan-2-ol. For the butan-1-ol isomers, larger solubility differences are observed in the IL-rich phase. The qualitative trend of increasing solubility for secondary and tertiary alcohols is correctly described but this behaviour is not adequately captured quantitatively by the model. The solubilities in the alcohol rich phase are, however, well described. Other examples are presented in the Supporting Information.

4.3. Vapour–liquid equilibria prediction

Some examples of the vapour-phase behaviour for several ionic liquid-alcohol systems were obtained from literature and are reported in Table 1. A comparison between the experimental data and the COSMO-RS predictions, using the BP/TZVP procedure and the ions and alcohols lower energy ions conformation was performed. The results are presented in Figs. 13–17 in the form of p–x_{IL} diagrams for each binary mixture investigated. As before the COSMO-RS calculations were made for a pseudobinary mixture where the cation and anion, with equal concentrations, are treated as separate species. The results obtained for the p–x_{IL} phase diagrams are discussed below from different points of view to evaluate the influence of the ILs structural variations and its dependence with tempera-

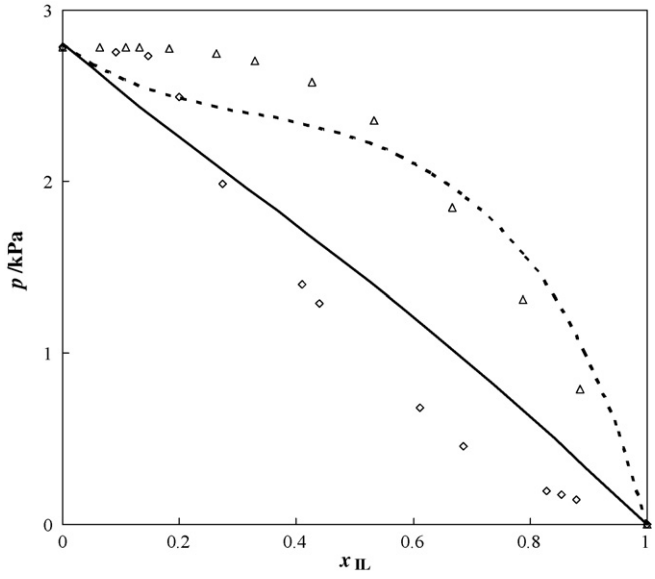

Fig. 13. Vapour–liquid phase diagram at 298.15 K [C_4mim][Tf_2N] (△) (- - -) and [C_4mim][OctS] (◊) (—) with propan-1-ol. The single symbols and the lines represent respectively the experimental data [31,26] and the COSMO-RS prediction calculations.

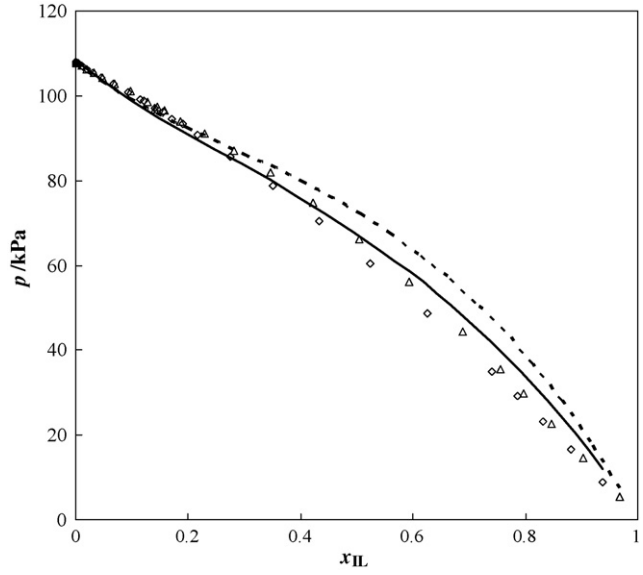

Fig. 15. Vapour–liquid phase diagram at 353 K for [C_2mim][Tf_2N] (△) (- - -) and [C_6mim][Tf_2N] (◊) (—) with ethanol. The single symbols and the lines represent respectively the experimental data [25] and the COSMO-RS prediction calculations.

ture and the COSMO-RS predictive capability. As expected the description of the VLE phase diagrams is superior to the LLE since they are easier to describe. Reasonable quantitative descriptions are easily achieved with COSMO-RS for the VLE binary systems studied unlike what was observed for some LLE systems.

4.3.1. Anion identity influence

Fig. 13 presents a comparison between the experimental data and COSMO-RS predictions for the p–x_{IL} phase diagram of [C_4mim][OctS] and [C_4mim][Tf_2N] with propan-1-ol at 298.15 K. The COSMO-RS prediction provides the correct tendency of the pressure increase with the anion [OctS] < [Tf_2N], allowing the speculation that [OctS]-based ILs will present higher miscibilities with alcohols than [Tf_2N]-based ILs. Although, the quantitative predictions provided by COSMO-RS present considerable deviations when compared to experimental data. The COSMO-RS seems to be able to describe better phase diagrams with strong positive deviations from Raoult's law, as observed for the [Tf_2N]-based ILs, but worst the negative deviations, as observed for the [OctS]-based

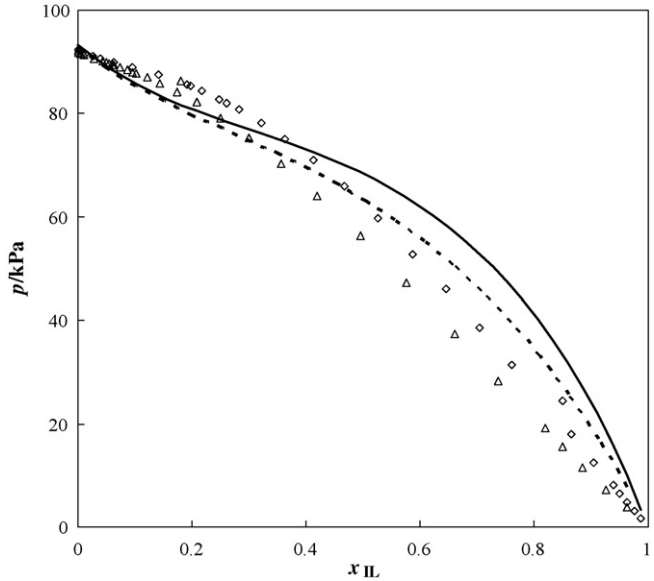

Fig. 14. Vapour–liquid phase diagram at 353.15 K for [C_2mim][Tf_2N] (◊) (—) and [C_4mim][Tf_2N] (△) (- - -) with propan-2-ol. The single symbols and the lines represent respectively the experimental data [24] and the COSMO-RS prediction calculations.

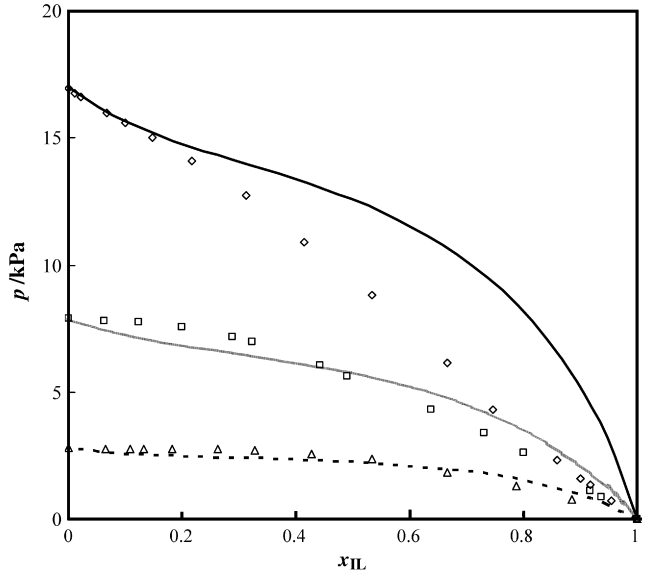

Fig. 16. Vapour–liquid phase diagram at 298.15 K for [C_4mim][Tf_2N] with methanol (◊) (—), ethanol (□) (▪▪▪▪) and propan-1-ol (△) (- - -). The single symbols and the lines represent respectively the experimental data [31] and the COSMO-RS prediction calculations.

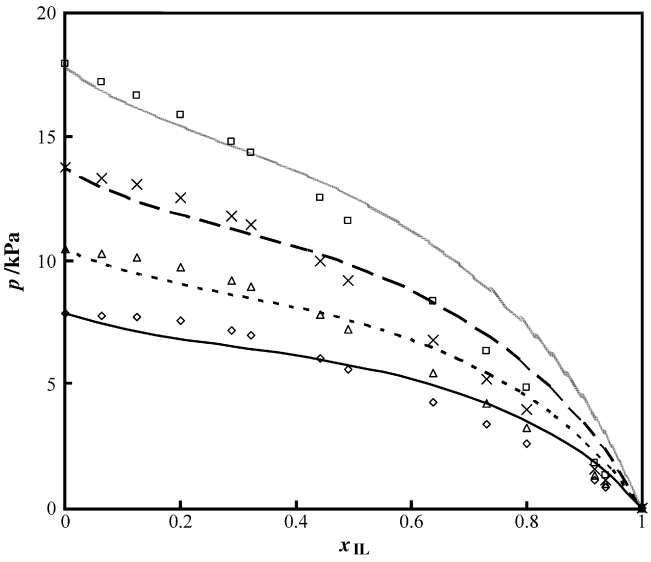

Fig. 17. Vapour–liquid phase diagram for [C_4mim][Tf_2N] and ethanol at isotherms: 298.15 K (◊) (—), 303.15 K (△) (- - -), 308.15 K (×) (– – –) and 313.15 K (□) (·····). The single symbols and the lines represent respectively the experimental data [31] and the COSMO-RS prediction calculations.

ILs. Results for other isotherms and with other alcohols are presented in the Supporting Information.

4.3.2. Cation alkyl chain length influence

Figs. 14 and 15 show the vapour–liquid phase behaviour for [C_2mim][Tf_2N] and [C_4mim][Tf_2N] with propan-2-ol at 353.15 K and [C_2mim][Tf_2N] and [C_6mim][Tf_2N] with ethanol at 353 K. The COSMO-RS predictions provide a good qualitative description of the p–x_{IL} phase diagram changes with the cation alkyl chain length. For VLE description, the increasing deviation of the COSMO-RS predictions with the alkyl chain length of the ILs is not as pronounced as for the LLE. Actually, the model seems to be able to adequately describe the increase of the positive deviation from Raoult's law with decreasing alkyl chain length.

4.3.3. Alcohol chain length influence

Fig. 16 shows the comparison between experimental data and COSMO-RS predictions for the vapour–liquid phase behaviour of [C_4mim][Tf_2N] in combination with alcohols of different alkyl chain length. The COSMO-RS correctly describes the vapour–liquid tendency and the Raoult's law positive deviation, where just a small overprediction of the positive deviation of Raoult's law appears for very short chain alcohols, such as methanol. This is also verified for all the isotherms under study and for similar systems with other combinations of cations and anions, as shown in some examples depicted in the Supporting Information. The worst descriptions of the phase equilibria observed for these systems result from the strong polarity of methanol, that COSMO-RS has some difficulties in capture.

4.3.4. Temperature dependence influence

In Fig. 17, the comparison between the experimental data and COSMO-RS predictions for the vapour–liquid phase behaviour at several isotherms for the [C_4mim][Tf_2N]—ethanol system is presented. COSMO-RS is able to correctly describe the vapour–liquid phase diagrams as a function of temperature. Although data in a larger temperature range would be required to fully establish the adequacy of the temperature dependence of the COSMO-RS predictions, the results here reported, along with other results presented in the Supporting Information and along with the LLE results, seem to indicate that COSMO-RS provides a correct temperature dependence of the liquid phase non-ideality.

4.4. Enthalpy of vaporization prediction for pure compounds

In order to address the increasing deviations in the predictions obtained with COSMO-RS for molecules with larger alkyl chains, the vaporization enthalpies of pure 1-alkanols and [$C_n$mim][Tf_2N] ILs were predicted and evaluated against experimental data [47,48]. A figure with both predicted and experimental vaporization enthalpies is provided in the Supporting Information of this manuscript.

Although the enthalpies of vaporization for the 1-alkanols seem to be adequately described and the correct chain length dependency is obtained, the predicted enthalpies of vaporization of the pure ionic liquids fail to describe the increase with the alkyl chain length observed experimentally. These results may explain the larger degradation of the LLE observed with increasing chain length as compared to the VLE, as for this type of equilibria the influence of the alkanol will be more important since they vaporize alone. The poor description of the enthalpies of vaporization for the ILs may reflect a poor description of the interactions in liquid phase, not only among the IL molecules, but also between the IL alkyl moieties and the alkyl chains of other compounds. As suggested above the problem with the description of the ionic liquids seems to arise from the IL microstructure formation [47] that it is not taken into account with the COSMO-RS calculations. Also, the COSMO-RS fails in estimating the methanol enthalpies of vaporization correctly, due to its strong polarity, explaining the failure in the VLE systems descriptions involving methanol as a solvent.

5. Conclusions

ILs have been suggested as potential "green" solvents to replace volatile organic solvents in reaction and separation processes due to their negligible vapour pressures. To design ILs for these applications, it is important to develop a predictive method capable of describing the changes in phase behaviour of such systems along with the structure of ILs and solvents.

Quantum chemical calculations based on the σ profiles of the cation, the anion, and the alcohol were used for the prediction of LLE and VLE binary systems of several imidazolium and pyridinium-based ILs and alcohols. COSMO-RS and its implementation in the program COSMOtherm are capable of giving a priori predictions of the systems thermodynamics involving ILs, which may be of considerable value for the extrapolation of suitable ILs for practical applications.

Although the results of COSMO-RS look promising, deviations from the LLE experimental data are observed especially for compounds with longer alkyl chains and from the VLE with methanol.

In spite of some shortcomings the COSMO-RS model provides a reasonable qualitative agreement with the experimental data for both LLE and VLE binary systems. Thus, in this study COSMO-RS proved to be a useful tool to scan the large number of possible ILs or to help in the design of new ILs for specific applications, since it allows the a priori prediction of their thermodynamic behaviour with common solvents. Nevertheless, it should be noted that COSMO-RS, at the present, is not able to treat ions correctly at finite low ionic strength due to the long-range ion-ion interactions involved, and besides the small effects it induces they must be considered, and much more experimental and theoretical work is needed to improve such type of predictions.

List of symbols

a_{eff}	effective contact area between two surface segments
A^{X_i}	total surface area of molecule X_i
c_{HB}	hydrogen bond strength coefficient
E_{HB}	hydrogen bonding energy
E_{misfit}	electrostatic misfit energy
E_{vdW}	van der Waals energy
p	pressure
$p_{\text{S}}(\sigma)$	sigma profile of a solvent
$p^{X_i}(\sigma)$	sigma profile of a solute i
$p'_{\text{S}}(\sigma)$	normalised sigma profile of a solvent
T	temperature
x_i	mole fraction of compound i
X_i	i molecule considered as solute
x_{IL}	ionic liquid mole fraction

Greek symbols

α'	electrostatic misfit interactions coefficient
σ	polarization charge density
σ_{acceptor}	polarization charge of an hydrogen bonding acceptor
σ_{donor}	polarization charge of an hydrogen bonding donor
σ_{HB}	hydrogen bonding threshold
τ_{vdW}	element-specific vdWs coefficient
τ'_{vdW}	element-specific vdWs coefficient

Acknowledgments

The authors thank financial support from Fundação para a Ciência e a Tecnologia (Project POCI/EQU/58152/2004) and Ph.D. grant (SFRH/BD/14134/2003) of Mara G. Freire. They also acknowledge F. Eckert and A. Klamt, COSMOtherm, Version C2.1, Release 01.05, COSMOlogic GmbH & Co. KG, Leverkusen, Germany, 2005, and M. Diedenhofen of COSMOlogic for advice and assistance in the use of COSMOtherm.

Appendix A. Supplementary data

Supplementary data associated with this article can be found, in the online version, at doi:10.1016/j.fluid.2007.04.020.

References

[1] M.J. Earle, J.M.S.S. Esperança, M.A. Gilea, J.N. Canongia Lopes, L.P.N. Rebelo, J.W. Magee, K.R. Seddon, J.A. Widegren, Nature 439 (2006) 831–834.
[2] J.G. Huddleston, H.D. Willauer, R.P. Swatloski, A.E. Visser, R.D. Rogers, Chem. Commun. 44 (1998) 1765–1766.
[3] J. McFarlane, W.B. Ridenour, H. Luo, R.D. Hunt, D.W. DePaoli, R.X. Ren, Sep. Sci. Technol. 40 (2005) 1245–1265.
[4] A.G. Fadeev, M.M. Meagher, Chem. Commun. 44 (2001) 295–296.
[5] T.M. Letcher, N. Deenadayalu, B. Soko, D. Ramjugernath, P.K. Naicker, J. Chem. Eng. Data 48 (2003) 904–907.
[6] J.M. Crosthwaite, S.N.V.K. Aki, E.J. Maggin, J.F. Brennecke, J. Phys. Chem. B 108 (2004) 5113–5119.
[7] J.M. Crosthwaite, S.N.V.K. Aki, E.J. Maggin, J.F. Brennecke, Fluid Phase Equilib. 228/229 (2005) 303–309.
[8] J.M. Crosthwaite, M.J. Muldoon, S.N.V.K. Aki, E.J. Maggin, J.F. Brennecke, J. Phys. Chem. B 110 (2006) 9354–9361.
[9] V. Najdanovic-Visak, J.M.S.S. Esperança, L.P.N. Rebelo, M. Nunes da Ponte, H.J.R. Guedes, K.R. Seddon, J. Szydlowskiy, J. Phys. Chem. B 107 (2003) 12797–12807.
[10] V. Najdanovic-Visak, J.M.S.S. Esperança, L.P.N. Rebelo, M. Nunes da Ponte, H.J.R. Guedes, K.R. Seddon, J. Szydlowskiy, J. Phys. Chem. Chem. Phys. 4 (2002) 1701–1703.
[11] V. Najdanovic-Visak, L.P.N. Rebelo, M. Nunes da Ponte, Green Chem. 7 (2005) 443–450.
[12] J. Łachwa, P. Morgado, J.M.S.S. Esperança, H.J.R. Guedes, J.N.C. Lopes, L.P.N. Rebelo, J. Chem. Eng. Data 51 (2006) 2215–2221.
[13] A. Heintz, D. Klasen, J.K. Lehmann, C. Wertz, J. Solution Chem. 34 (2005) 1135–1144.
[14] A. Heintz, J.K. Lehmann, C. Wertz, J. Chem. Eng. Data 48 (2003) 274–472.
[15] A. Heintz, J.K. Lehmann, C. Wertz, J. Jacquemin, J. Chem. Eng. Data 50 (2005) 956–960.
[16] U. Domańska, E. Bogel-Łukasik, R. Bogel-Łukasik, Chem. Eur. J. 9 (2003) 3033–3041.
[17] U. Domańska, Thermochim. Acta 448 (2006) 19–30.
[18] U. Domańska, E. Bogel-Łukasik, Ind. Eng. Chem. Res. 42 (2003) 6986–6992.
[19] U. Domańska, A. Pobudkowska, F. Eckert, J. Chem. Thermodyn. 38 (2006) 685–695.
[20] K.N. Marsh, A.V. Deev, A.C.-T. Wu, E. Tran, A. Klamt, Korean J. Chem. Eng. 19 (2002) 357–362.
[21] C.-T. Wu, K.N. Marsh, A.V. Deev, J.A. Boxal, J. Chem. Eng. Data 48 (2003) 486–491.
[22] K. Sahandzhieva, D. Tuma, S. Breyer, A.P.-S. Kamps, G. Maurer, J. Chem. Eng. Data 51 (2006) 1516–1525.
[23] R. Kato, J. Gmehling, Fluid Phase Equilibr. 227 (2005) 255–266.
[24] R. Kato, J. Gmehling, Fluid Phase Equilibr. 231 (2005) 38–43.
[25] R. Kato, J. Gmehling, J. Chem. Thermodyn. 37 (2005) 603–619.
[26] J. Safarov, S.P. Verevkin, E. Bich, A. Heintz, J. Chem. Eng. Data 51 (2006) 518–525.
[27] A. Heintz, T.V. Vasiltsova, J. Safarov, E. Bich, S.V. Verevkin, J. Chem. Eng. Data 51 (2006) 648–655.
[28] N. Calvar, B. González, E. Gómez, A. Domínguez, J. Chem. Eng. Data 51 (2006) 2178–2181.
[29] M. Bendová, Z. Wagner, J. Chem. Eng. Data 51 (2006) 2126–2131.
[30] X. Hu, J. Yu, H. Liu, J. Chem. Eng. Data 51 (2006) 691–695.
[31] S.P. Verevkin, J. Safarov, E. Bich, E. Hassel, A. Heintz, Fluid Phase Equilibr. 236 (2005) 222–228.
[32] H.C. de Sousa, L.P.N. Rebelo, J. Polym. Sci. B: Polym. Phys. 38 (2000) 632–651.
[33] A. Shariati, C.J. Peters, J. Supercrit. Fluids 25 (2003) 109–111.
[34] L.P.N. Rebelo, J.N.C. Lopes, J.M.S.S. Esperança, E. Filipe, J. Phys. Chem. B 109 (2005) 6040–6043.
[35] A. Klamt, J. Phys. Chem. 99 (1995) 2224–2235.
[36] F. Eckert, A. Klamt, AIChE J. 48 (2002) 369–385.
[37] A. Klamt, F. Eckert, Fluid Phase Equilibr. 172 (2000) 43–72.

[38] A. Klamt, COSMO-RS from quantum chemistry to fluid phase thermodynamics and drug design, Elsevier, Amsterdam, 2005.
[39] U. Domańska, A. Pobudkowska, F. Eckert, Green Chem. 8 (2006) 268–276.
[40] M.G. Freire, L.M.N.B.F. Santos, I.M. Marrucho, J.A.P. Coutinho, Braz. J. Chem. Eng. (2007) accepted for publication.
[41] T. Banerjee, M.K. Singh, A. Khanna, Ind. Eng. Chem. Res. 45 (2006) 3207–3219.
[42] F. Eckert, A. Klamt, COSMOtherm. Version C2.1, Release 01.05, COSMOlogic GmbH & Co. Kg, Leverkusen, Germany, 2005.
[43] F. Eckert, COSMOtherm user's manual version C2.1, Release 01.05, COSMOlogic GmbH & Co. Kg, Leverkusen, Germany, 2005.
[44] A. Schäfer, A. Klamt, D. Sattel, J.C.W. Lohrenz, F. Eckert, Phys. Chem. Chem. Phys. 2 (2000) 2187–2193.
[45] R. Ahlrichs, M. Bär, M. Häser, H. Horn, C. Kölmel, Chem. Phys. Lett. 162 (1989) 165–169.
[46] A. Schäfer, C. Huber, R. Ahlrichs, J. Chem. Phys. 100 (1994) 5829–5835.
[47] L.M.N.B.F. Santos, J.N.C. Lopes, J.A.P. Coutinho, J.M.S.S. Esperança, L.R. Gomes, I.M. Marrucho, L.P.N. Rebelo, J. Am. Chem. Soc. 129 (2007) 284–285.
[48] NIST Chemistry WebBook at http://webbook.nist.gov/chemistry/.